Z. Phys. Chem. **217** (2003) 1399–1410

Establishment of Micellar Catalytic Field Using the *p*-Nitro-*o*-Carboxylbenzeneazo-8-Aminoquinoline – Cetyltrimethylammonium Bromide – Co(II) Ternary Complexation

By Hong-Wen Gao[1,*], Jia-Xiang Yang[2], and Jian-Fu Zhao[1]

[1] State Key Laboratory of Pollution Control and Resources Reuse, School of Environmental Science and Engineering, Tongji University, Shanghai-200092, P.R. China
[2] School of Chemistry and Chemical Engineering, Anhui University, Hefei-230039, P.R. China

(Received June 29, 2003; accepted August 26, 2003)

MSASC Technique / Micellar Catalytic Field / Cetyl Trimethylammonium Bromide / p-Nitro-o-Carboxylbenzeneazo-8-Amino-Quinoline / Cobalt

The micellar catalytic field was proposed in surfactant medium by investigating the complexation between *p*-nitro-*o*-carboxylbenzeneazo-8-aminoquinoline (NCBAAQ) and Co(II) at pH 8.8. The cationic surfactant, cetyl trimethylammonium bromide (CTAB) was added and the aggregation of NCBAAQ on CTAB obeys the Langmuir isothermal adsorption. The enrichment of NCBAAQ on CTAB micelle resulted in a sensitive and rapid complexation of NCBAAQ with Co(II). The ternary complexation was characterized by the microsurface adsorption – spectral correction (MSASC) technique. Results showed that the complex $Co_3NCBAAQ_{12}CTAB_{78}$ is formed.

1. Introduction

Surfactants (S) are often very useful in trace analysis [1, 2] and element separation [3–5] because of its synergism, *e.g.* solubilization, stabilization and sensitization. The synergism mechanisms include micelle extraction, synergism perturbation [6], hydrogen bond formation [7], micelle catalysis [8], asymmetric microenvironment [9] and so on. However, each of all them has a limitation. How to reasonably explain the synergism of any surfactant, we are trying to propose a novel mechanism named micellar catalytic

---

[*] Corresponding author. E-mail: hwgao@mail.tongji.edu.cn

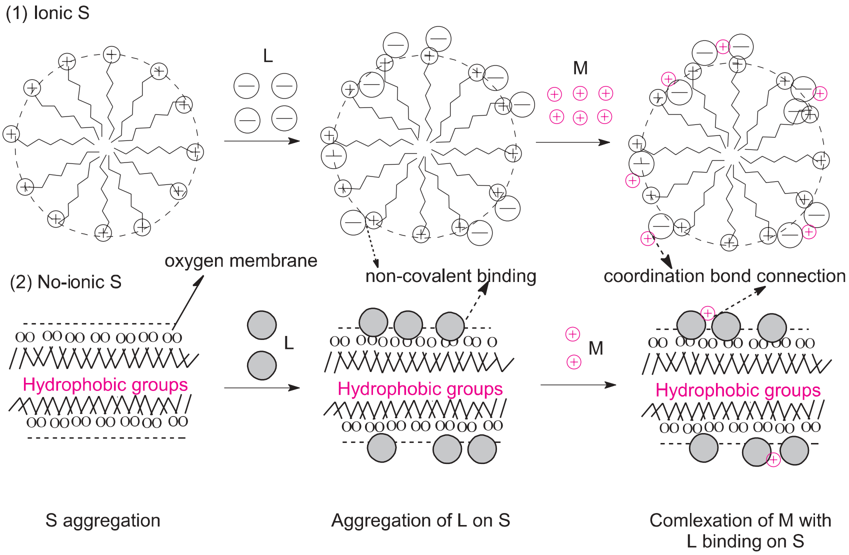

Fig. 1. The adsorption of ligand (L) molecules on surfactant (S) monomer (1) and micelle (2) surface and the sensitive complexation of a metal (M) with L adsorbed on S surface.

field for any ionic or non-ionic surfactant. To see the sketch Fig. 1, the self-aggregation of ionic surfactant molecules will form a strongly electrostatic global micelle and that of non-ionic surfactant molecules form a two-layer micelle where a great deal of the strongly polar oxygen distribute on the H_2O – micelle contact surface to form a weakly electrostatic body. Thus, ionic surfactant can attract oppositely charged molecules (L) and non-ionic surfactant attract positively charged molecules on H_2O-micelle connect surface or non-polar molecules into the two-layer. After the electrostatic attraction, the non-covalent co-action of the hydrogen bond, hydrophobic bond, ver de Waal force and molecular winding make the interaction between S and L firm. The enrichment of L on S microsurface results in a rapid and easy complexation with a metal ion (M). Thus, S micelle provides the complexation between M and L with a catalytic reaction field. Interestingly, the aggregation of L on S accords with the Langmuir isothermal adsorption [10, 11]. Therefore, the non-covalent interaction between S and L is in only one monolayer. Spectrometry is a conventional method to characterize the molecular interaction [12, 13]. Because the non-covalent interaction is always weaker than a covalent bond connection, the absorption spectrum of the aggregation product has often only a little shift. Thus, ordinary spectrophotometry is limited because of the interference of excess of L in aqueous medium. The spectral correction technique developed early [14] has been applied in this work. The combination of the microsurface adsorption and the spectral correction technique provides the study of the ternary complexation with a useful approach. The following relations were used [15]:

$$\frac{1}{\gamma} = \frac{1}{N} + \frac{1}{KNC_{\mathrm{L}}} \tag{1}$$

$$\gamma = \eta \frac{C_{\mathrm{L0}}}{C_{\mathrm{S}}} \tag{2}$$

$$C_{\mathrm{L}} = (1-\eta)C_{\mathrm{L0}} \tag{3}$$

where

$$\eta = \frac{A_{\mathrm{C}} - \Delta A}{A_0} \tag{4}$$

where K is the binding constant and C_{L} the molar concentration of excess of L. γ is the molar ratio of L to S and N indicates maximal binding number of L. C_S and C_{L0} are the concentrations of the S and L added initially and η indicates the effective fraction of L. A_{C}, A_0 and ΔA are the real absorbance of the S–L product, the absorbance of L measured against water and that of the S–L solution against L measured at wavelength λ_2. From linear γ^{-1} *vs.* C_{L}^{-1} is linear, N and K were calculated. A_{C} is calculated by means of [15]:

$$A_{\mathrm{c}} = \frac{\Delta A - \beta \Delta A'}{1 - \alpha\beta} \tag{5}$$

where $\Delta A'$ indicates the absorbance of the S–L solution measured at wavelength λ_1. α and β are correction constants. In addition, the molar absorptivity (real $\varepsilon_{\mathrm{r}}^{\lambda 2}$ not apparent $\varepsilon_{\mathrm{a}}^{\lambda 2}$) of the adsorption product $\mathbf{SL}_{\boldsymbol{N}}$ at λ_2 is calculated by the following equation:

$$\varepsilon_{\mathrm{r}}^{\lambda 2} = \frac{mNA_c}{\delta \gamma C_{\mathrm{S}}} \tag{6}$$

where δ is the cell thickness (cm) and the others have the same meanings as in the equations above.

The following equation [16] was used to calculate the n-th step stability constant (K_n) of a metal complex ML_N (M-metal ion).

$$K_n = \frac{\gamma + 1 - n}{(n-\gamma)(C_{\mathrm{L}} - \gamma C_{\mathrm{M}})} \tag{7}$$

where n indicates the step number of complex and the other symbols have the same meanings with those above. The cumulative constant (K) of complex

ML_N is calculated by the following expression: $K = K_1 \times K_2 \times \ldots \times K_n \ldots \times K_N$. The n-th step real (not apparent) absorptivity $\left(\varepsilon_{MLn}^{\lambda 2}\right)$ of a metal complex is calculated by the relation [16]:

$$\varepsilon_{MLn}^{\lambda 2} = \frac{A_C}{\delta C_M(\gamma' + 1 - n)} - \frac{n - \gamma'}{\gamma' + 1 - n}\varepsilon_{MLn-1}^{\lambda 2} \tag{8}$$

where $\varepsilon_{MLn-1}^{\lambda 2}$ indicates the $n-1$-th step absorptivity of complex and the others have the same meanings as in the equations above.

In the present work, we have studied the interaction of cetyltrimethylammonium bromide (CTAB) with *p*-nitro-*o*-carboxyl- benzeneazo-8-aminoquinoline (NCBAAQ) and the complexation of Co(II) with NCBAAQ in micelle medium. The synthesis of the dye ligand, NCBAAQ was made and its structure is given below:

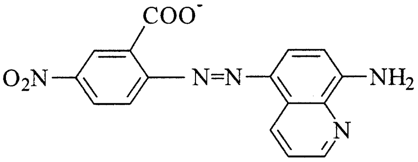

p-nitro-*o*-carboxyl-benzeneazo-8-aminoquinoline (NCBAAQ)

It forms monovalent anion in neutral medium and it can bind on CTAB. Results have shown that the binding ratio of CTAB to NCBAAQ is 2:1 and the binding constant of the CTAB-NCBAAQ complex is $K_{\text{CTAB-NCBAAQ}} = 2.99 \times 10^5\ \text{l}\,\text{mol}^{-1}$. The ternary complexation among CTAB, NCBAAQ and Co(II) has been characterized.

2. Experimental section

2.1 Apparatus and reagents

Absorption spectra were recorded on a TU1901 Spectrophotometer (PGeneral, Beijing) and independent absorbance was measured on a Model 722 spectrophotometer. DDS-11A conductivity meter, (Tianjin Second Analytical Instruments) was used to measure conductivity together with DJS-1 conductivity immersion electrode (electrode constant 0.98) (Shanghai Tienkuang Devices) in product of non-ionic water of $< 0.5\ \mu\Omega^{-1}\ \text{cm}^{-1}$. The pH of the solution was measured with a pHS-2C acidity meter (Leici Instruments, Shanghai, China) and Model 630D pH Pen (Shanghai Ren's Electronic). The temperature was adjusted and remained constant in a Model 116R electrically heated thermostatic bath, (Changjiang Test Instruments of Tongjiang, China).

Standard stock solution of CTAB (10.00 mmol/l) was prepared by dissolving CTAB (Shanghai Chemical Reagents Center) in de-ionized water and then the CTAB use solution (1.00 mmol/l) was prepared daily by diluting the stock solution. The NCBAAQ solution (2.00 mmol/l) was prepared by dissolving 0.3360 g of NCBAAQ (it was synthesized below.) in 500 ml of DMF. The CTAB-NCBAAQ aggregate solution (0.800 mmol/l) was prepared by mixing 40.0 ml of NCBAAQ (2.00 mmol/l), 50.0 ml of the CTAB use solution (10.0 mmol/l) and 10.0 ml of pH 8.8 buffer solution. This solution contains the micellar aggregate, 0.0667 mmol/l $NCBAAQ_{12}CTAB_{78}$, where the free NCBAAQ approaches zero. Standard stock Co(II) solution [100.0 μg Co/ml (= 1.67 μmol Co/ml)] was prepared by dissolving 0.1000 g of pure cobalt metal (content $>$ 99.95%) in 10 ml of HNO_3 solution $(1+1)$ and then diluting to 1000 ml with deionized water. Standard Co(II) use solution (10.00 μg/ml) was prepared by diluting the above solution. The borax–boric acid buffer solutions (between pH 7.5 and 11.4) and NaOH solution (1.0 mol/l) were used to adjust the acidity of the solution. The NaCl solution (2.0 mol/l) was used to adjust the ionic strength of the aqueous solutions. All reagents were of analytical grade and used without further purification except for NCBAAQ.

3. General procedures

Synthesis of NCBAAQ [17]: The synthesis of the dye ligand NCBAAQ was made in our laboratory according to the following way.

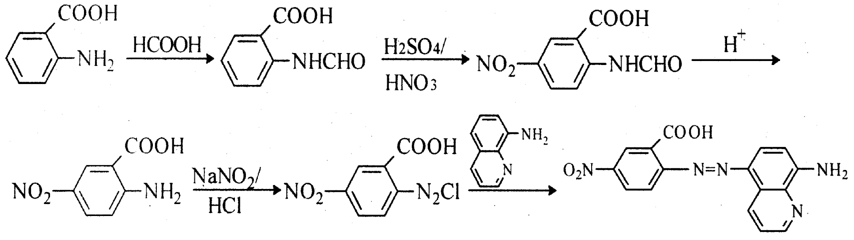

p-nitro-*o*-carboxyl-benzeneazo-8-aminoquinoline (NCBAAQ)

The final product must be recrystallized and purified in DMF to obtain pure NCBBQ, content of which was more than 98%.

Interaction of CTAB-NCBAAQ: Into a 25 ml calibrated flask were added 1.00 ml of CTAB work solution, 2.5 ml of buffer solution and an appropriate volume of the NCBAAQ solution (2.00 mmol/l). The solution was diluted to 25 ml with de-ionized water and mixed thoroughly. After 10 min, the ab-

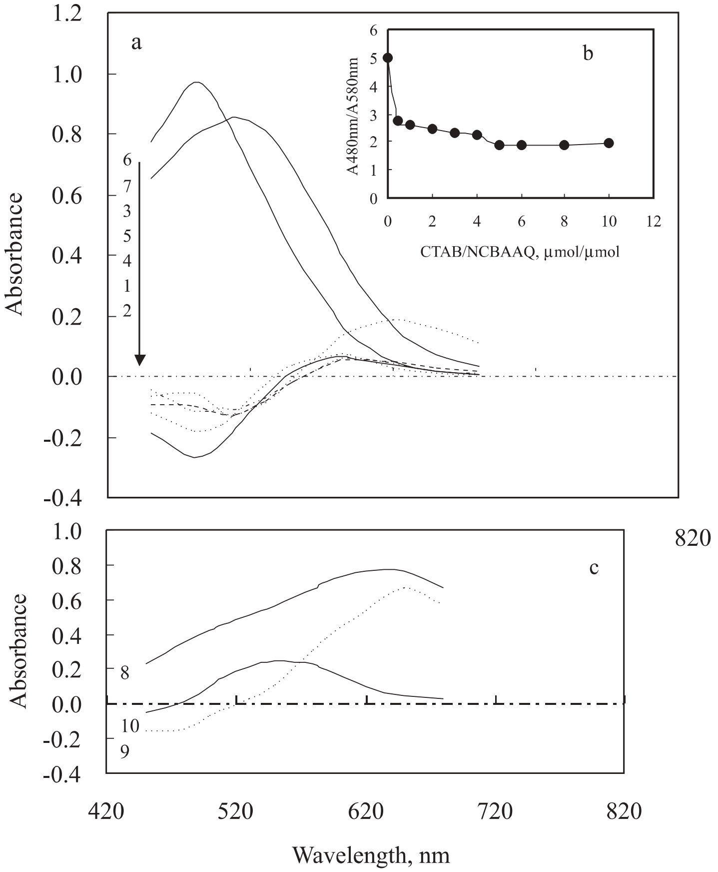

Fig. 2. Absorption spectra of NCBAAQ, NCBAAQ-CTAB and Co-NCBAAQ-CTAB solutions at pH 8.8: a-1- NCBAAQ (1.00 μmol)–CTAB (2.00 μmol) solution at pH 8.0; a-2-, a-3-, a-4- and a-5- same as a-1- but at pH 8.8, 9.6, 11.4 and 13.5; a-6- NCBAAQ (1.00 μmol) solution at pH 8.8; a-7- NCBAAQ (0.50 μmol)–CTAB (3 μmol) solution at pH 8.8; b- Effect of the initial molar ratio of CTAB to NCBAAQ on the ratio of the absorbances of solution measured at 480 and 580 nm; c-8- Co(8.5 μmol)–NCBAAQ-CTAB product (0.80 μmol) solution, c-9- NCBAAQ-CTAB aggregate (0.80 μmol)–Co (0.170 μmol) solution, and c-10- same as c-9- but in absence of CTAB. Curves a-6-, a-7 and c-8 against water and the others against the reagent blank.

sorbances were measured at 480 and 580 nm, respectively against the reagent blank treated in the same way without CTAB, and A_C of the binary adsorption aggregate was calculated.

Interaction of Cobalt-CTAB-NCBAAQ: In a 25 ml flask, added 2.5 ml of pH 8.8 buffer solution and an appropriate volume of the CTAB-NCBAAQ aggregate solution (0.0667 mmol/l). After 10 min, added 10 μg (0.167 μmol) of Co(II). Diluted to 25 ml and mixed well. After 15 min, the absorbances were measured at 480 and 650 nm, respectively against a reagent blank without Co(II) and A_C of the ternary complex was calculated.

4. Results and discussion

4.1 Spectral analysis

The interaction of NCBAAQ with CTAB: The absorption spectra of the CTAB-NCBAAQ solutions are shown in Fig. 2(a), where 2.00 μmol of CTAB and 0.500 μmol of NCBAAQ were added. From curves 1, 2, 3, 4 and 5, all of their peak and valley are located at 580 and 480 nm but curves 1, 2 and 3 show the higher absorbances. So pH 8.8 buffer solution was added in this work. From curve 6, the absorption peak of NCBAAQ is located at 480 nm. Fig. 2(b) shows the change of absorbance ratio, A480 nm/A580 nm of the NCBAAQ-CTAB solution with CTAB molar concentration. The ratio approaches a minimum when CTAB is over 5 times NCBAAQ. Therefore, the solution containing 6.0 μmol of CTAB and 1.0 μmol of NCBAAQ no longer contains free NCBAAQ. Curve 7 shows the absorption spectrum of such a solution and its absorption peak is located at 520 nm. By comparison of curves 6 and 7, the spectral red shift of the aggregate is only 40 nm. However, from the relative spectrum 2, the peak is located at 580 nm and the valley at 480. Such two wavelengths were used in this work. From curves 6 and 7, the correction constants were calculated to be $\beta = 0.197$ and $\alpha = 1.85$. Therefore, the real absorbance of the CTAB-NCBAAQ aggregate is calculated by $A_C = 1.57(\Delta A - 0.197\,\Delta A')$.

The complexation between NCBAAQ *and* Co(II): Into the CTAB-NCBAAQ aggregate solution, Co(II) was added. Co(II) can complex NCBAAQ binding on the CTAB-NCBAAQ aggregate. Its absorption spectra are shown in Fig. 2(c). From curve 8, the absorption of the ternary complex is located at 640 nm. By comparison of curves 7 and 8, the spectral red shift of the complex reaches 120 nm. It indicates that the coordination bond connection of Co with NCBAAQ results in a much longer spectrum shift than the non-covalent binding of NCBAAQ on CTAB. Therefore, the non-covalent binding is weaker than the chemical bond. By comparing curve 9 with 10, the absorption peak and valley of the CTAB-NCBAAQ-Co solution are much higher than those of the NCBAAQ-Co solution without CTAB. This is attributed to the sensitization of CTAB micelles. From curve 9, such two wavelengths 480 nm (absorption valley) and 650 nm (absorption peak) were selected in characterization of the ternary complex. From curves 8 and 9, the correction constants were calculated to be $\beta = 0.045$ and $\alpha = 0.460$. Therefore, the real absorbance of the ternary complex was calculated by $A_C = 1.02(\Delta A - 0.045\Delta A')$.

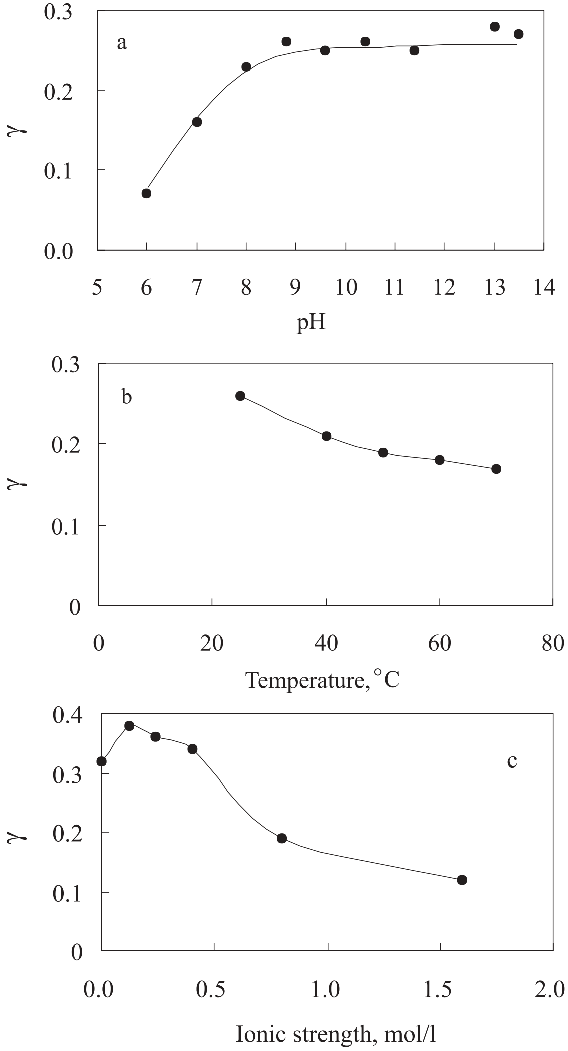

Fig. 3. Effect of pH (a), temperature (b) and ionic strength (c) on the binding ratio γ of NCBAAQ to CTAB (solution containing 1.00 μmol of NCBAAQ and 2.00 μmol of CTAB).

4.2 Effect of pH, temperature and ionic strength

By varying pH of the solution, the absorbance of the CTAB-NCBAAQ solutions was measured and γ of NCBAAQ to CTAB is shown in Fig. 3(a). γ decreases with increase of acidity of the solution. When pH is over 8.0, the binding ratio approaches a maximum. In order to avoid the precipitation of

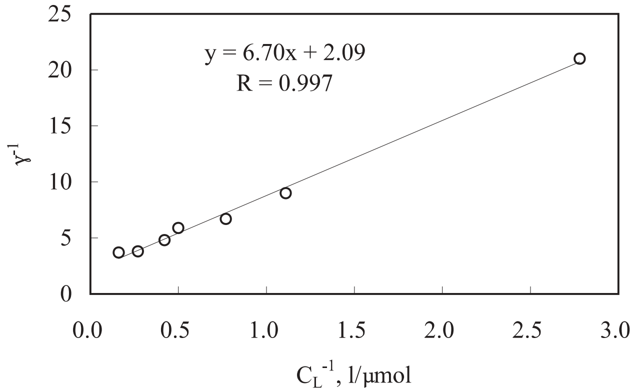

Fig. 4. γ^{-1} *vs.* C_L^{-1}.

Co(II) in strong basic solution, pH 8.8 buffer solution was added in this work. The anion $NCBAAQ^-$ can be formed at pH 8.8.

The effect of temperature on γ of NCBAAQ to CTAB is shown in Fig. 3(b). γ decreases by about 10% per increasing 10 °C. This is attributed to the fact that a weak non-covalent interaction could be destroyed by a high temperature [11].

In order to investigate the effect of ionic strength on the aggregation of NCBAAQ on CTAB, 2.0 mol/l NaCl was added and its affect is shown in Fig. 3(c). Between 0 and 0.5 mol/l, increase of the ionic strength is helpful to improve the interaction sensitivity because of increase γ. At 0.5 mol/l of ionic strength, γ approaches a maximum but then decreases rapidly. This is attributed to the fact that much more Cl^- than NCBAAQ began to bind on CTAB in replace of NCBAAQ.

4.3 Characterization of the aggregation

The aggregation of NCBAAQ *on* CTAB: Into 0.080 mmol/l CTAB, various volumes of the NCBAAQ solution were added. Both C_L and γ of each were calculated and plots C_L^{-1} *vs.* γ^{-1} is shown in Fig. 4. Because of the good linearity, the aggregation of NCBAAQ on CTAB accords with the Langmuir isothermal adsorption. From the linear intercept, the maximal binding number of NCBAAQ on CTAB is calculated to be $N = 0.5$. Therefore, the monomer aggregate is expressed as follows: $NCBAAQ \cdot CTAB_2$. The large micellar aggregate, $NCBAAQ_{39}CTAB_{78}$ (78-CMC of CTAB) could be formed when CTAB is more than CMC and NCBAAQ is excessive enough. From the linear slope, the binding constant of the aggregate was calculated to be $K = 2.99 \times 10^5\ \mathrm{l\,mol^{-1}}$. In addition, the real (not apparent) molar absorptivity of the micellar aggregate, $NCBAAQ_{39}CTAB_{78}$ was calculated to be $\varepsilon_r^{580\ \mathrm{nm}} = 3.52 \times 10^5\ \mathrm{l\,mol^{-1}\,cm^{-1}}$.

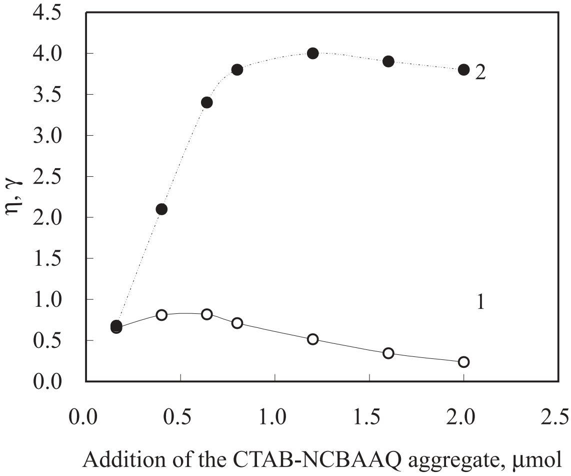

Fig. 5. Effect of addition of the NCBAAQ-CTAB aggregate on its effective fraction η (1) and the complex ratio γ of NCBAAQ to Co (2) [solution containing 10 μg of Co(II) at pH 8.8].

The complexation between NCBAAQ *and* Co(II): By varying the addition of 0.0667 mmol/l NCBAAQ-CTAB aggregate, the Co-NCBAAQ-CTAB ternary solutions were measured. η of the NCBAAQ-CTAB aggregate and γ of NCBAAQ to Co were calculated. Their curves are shown in Fig. 5. From curve 2, γ approaches a maximum at 4 when the addition of the NCBAAQ-CTAB aggregate solution is over 1.0 ml. Therefore, the ternary complex is $Co_3NCBAAQ_{12}CTAB_{78}$. From curve 1, only 51% of the NCBAAQ-CTAB aggregate bound on CTAB so 49% is still free in solution. Certainly, such a much excess of the CTAB-NCBAAQ aggregate affects the measurement of absorbance of the complex.

Determination of K_n *and* ε_n: The following solutions were prepared for the determination of the stability constant (K) and the real absorptivity (ε) of the

Table 1. Determination of A_C and γ of complex $(Co\cdot NCBAAQ_4\cdot CTAB_8)_{10}$ and calculation of the stepwise stability constant and real absorptivity at 25 °C.

n-step	Real abs. A_C	Effective molar ratio, γ	Stability constant, K_n ($\times 10^5$)	Real absorptivity, ε_n ($\times 10^4$ l mol^{-1} cm^{-1}) at 650 nm
1	0.070 ± 0.009	0.471 ± 0.022	2.54 ± 0.34	2.25 ± 0.11
2	0.234 ± 0.010	1.31 ± 0.002	1.22 ± 0.12	6.14 ± 0.28
3	0.496 ± 0.010	2.42 ± 0.030	1.06 ± 0.17	8.97 ± 0.47
4	0.708 ± 0.019	3.45 ± 0.070	0.84 ± 0.21	14.2 ± 0.67

Co-NCBAAQ complex in the presence of CTAB: 10.0 μg of Co(II) with 0.200, 0.400, 0.700 and 1.00 μmol of the NCBAAQ-CTAB aggregate. Six replicated determinations of each were carried out. A_{C}, γ, K_n and ε_n of the complex were calculated and the results are shown in Table 1. K decreases and ε increases with increase of n so it accords with the common chemical reaction law. The cumulative constant of the NCBAAQ-Co complex was calculated to be $K = 2.78 \times 10^{20}$.

In the determination of the formation constants of a complex, the spectral correction technique is simple in operation and easily understandable in principle over the classical methods such as continuous variations [18] and equilibrium movements [19].

5. Conclusion

Study on surfactant is always active [20–24]. Understanding the aggregation of small organic molecules on its micelle is significant to synthesize a new type of efficient surfactants and to select a suitable surfactant in trace analysis and element separation. The aggregation of L on S provides the complexation between M and L with a micellar catalytic field. It explained qualitatively the synergism of S in aqueous medium such as solubilization, sensitization and stabilization and characterized quantitatively its binding with L and M by MSASC technique. Though this work selected only an ionic surfactant, we described the basic physics behind the MSASC technique and surveyed some ongoing research on *e.g.* synergism of on-ionic surfactant, a mixed action of various surfactants, non-covalent modification of polymer and identification of protein structure.

References

1. M. Safavi, H. Abdollahi, F. Sedaghatpour, and M. R. Hormozi Nezhad, Talanta **59** (2003) 147.
2. S. Kundu, S. K. Ghosh, M. Mandal, T. Pal, and A. Pal, Talanta **58** (2002) 935.
3. C. Z. Katsaounos, D. L. Giokas, A. G. Vlessidis, E. K. Paleologos, and M. I. Karayannis, Sci. Total Environm. **305** (2003) 157.
4. A. Ito, S. Nii, F. Kawaizumi, and K. Takahashi, Separation Purif. Technol. **30** (2003) 139.
5. S. Tixier, M. Adamcyk, E. C. Young, J. H. Schmid, and T. Tiedje, J. Crystal. Growth **251** (2003) 449.
6. Y. X. Ci and M. M. Yang, Chin. Sci. Bull. **16** (1983) 980.
7. Y. X. Zheng, L. D. Li, and S. Q. Sun, Huaxue Shiji **6** (1984) 273.
8. B. Savvins, P. K. Chernova, and I. L. M. Kudpatseva, Zh. Anal. Khim. **33** (1978) 2127.
9. W. B. Qi and L. Z. Zhu, Chem. J. Chin. Univ. **7** (1986) 407.
10. I. Langmuir, J. Am. Chem. Soc. **40** (1918) 1361.
11. H. W. Gao and W. Q. Xu, Anal. Chim. Acta **458** (2002) 417.

12. A. Sanz-Medel, M. R. F. Campa, E. B. Gonzalez, and M. L. Fernandez-Sanchez, Spectrochim. Acta Part B: Atom. Spectrosc. **54** (1999) 251.
13. W. Wang and J. C. T. Kwak, Colloids Surf. A: Physicochem. Engineer. Aspects **156** (1999) 95.
14. H. W. Gao, Recl. Trav. Chim. Pays-Bas **114** (1995) 61.
15. H. W. Gao, J. AOAC Intern. **84** (2001) 532.
16. H. W. Gao, Talanta **52** (2000) 817.
17. J. M. Xu, T. S. Zhang, W. B. Tang *et al*., Chin. J. Chem. Reagents **21** (1999) 93.
18. W. Likussar, Anal. Chem. **45** (1973) 1926.
19. A. I. Laearev, Zavod. Lab. **41** (1975) 534.
20. R. Zana and Y. Talmon, Nature **362** (1993) 229.
21. A. Knaebel, R. Oda, E. Mendes *et al*., Langmuir **16** (2000) 2489.
22. R. Oda, I. Huc, and S. J. Candau, Chem. Commun. (1997) 2105.
23. S. Oszwaldowski, Colloids Surf. A: Physicochem. Engineer. Aspects **214** (2003) 287.
24. L. Besra, D. K. Sengupta, S. K. Roy, and P. Ay, Intern. J. Mineral Process. **66** (2002) 203.